Semicond. Sci. Technol. 27 (2012) 125013 (5pp) doi:10.1088/0268-1242/27/12/125013

Characterization of thin polycrystalline silicon films deposited on glass by CVD

A G Benvenuto[1], R H Buitrago[1,2], A Bhaduri[3], C Longeaud[3] and J A Schmidt[1,2]

[1] Instituto de Desarrollo Tecnológico para la Industria Química (INTEC), CONICET-UNL, Güemes 3450, S3000GLN Santa Fe, Argentina
[2] Facultad de Ingeniería Química, UNL, Santiago del Estero 2829, S3000AOM Santa Fe, Argentina
[3] Laboratoire de Génie Electrique de Paris, CNRS UMR 8507, Plateau de Moulon, 11 rue Joliot Curie, F-91190 Gif sur Yvette, France

E-mail: jschmidt@intec.unl.edu.ar

Received 8 August 2012, in final form 10 October 2012
Published 5 November 2012
Online at stacks.iop.org/SST/27/125013

Abstract

We deposited polycrystalline silicon (poly-Si) thin films on commercial float glass by chemical vapour deposition from trichlorosilane at temperatures between 735 and 870 °C. The structural properties of the films were evaluated by means of scanning electron microscopy, x-ray diffraction, atomic force microscopy, reflectance in the ultraviolet region and Raman spectroscopy. The electrical characterization involved measurements of dark conductivity and photoconductivity as a function of temperature, Hall effect, ambipolar diffusion length from the steady-state photocarrier grating technique and density of defects by means of modulated photoconductivity. By using boron tribromide as a doping agent, degrees of doping ranging from intrinsic to clearly p-doped were obtained. The process, the reactants and the substrate used are of low cost, and proved to be adequate for direct poly-Si deposition, giving films of good structural and electrical properties.

(Some figures may appear in colour only in the online journal)

1. Introduction

Thin polycrystalline silicon (poly-Si) layers deposited on glass substrates have attracted considerable attention as a base material to produce active-matrix liquid crystal displays, active-matrix organic light-emitting diodes and solar cells [1, 2]. Moreover, the luminescence properties of silicon nanocrystals have opened a wide range of exciting possibilities [3–5]. Several methods of poly-Si preparation have been developed, such as deposition of an amorphous film followed by crystallization, layer transfer methods or direct growth by chemical vapour deposition (CVD). In this last process, a Si-containing source gas is decomposed in several possible ways such as plasma (PECVD), catalysis (HWCVD) or thermally (CVD).

In order to develop a low-cost process that can be transferred to an industrial scale, a careful choice of the deposition process, the reactants and the substrate is essential. Atmospheric pressure thermal chemical vapour deposition (AP-CVD), using trichlorosilane ($SiHCl_3$) as a source gas and float glass as a substrate, appears as an optimum combination from the point of view of cost. AP-CVD allows high deposition rates, high uniformity, controllable doping profiles and good film quality with a relatively simple setup [6]. $SiHCl_3$ is an intermediate product in the production of feedstock silicon, and is much cheaper than other source gases such as silane. Finally, float glass is an excellent substrate since it combines low cost, transparency (to deposit the devices in a superstrate configuration), electrical insulation in large sheets (to use a monolithic interconnection scheme) and a thermal expansion coefficient matching that of silicon [2].

In a previous work [7], we have shown that a commercial aluminosilicate glass (Schott AF37 [8]) can be used as a substrate to deposit poly-Si by AP-CVD from $SiHCl_3$ at intermediate temperatures between 735 and 870 °C. By using boron tribromide (BBr_3) as a doping agent, degrees of doping ranging from intrinsic to clearly p-doped were obtained. The structural properties of the films were evaluated by means of scanning electron microscopy (SEM), atomic force

 © 2012 IOP Publishing Ltd Printed in the UK & the USA

microscopy (AFM), x-ray diffraction and reflectance in the ultraviolet region. We achieved acceptable deposition rates, obtaining films with high crystallinity and a columnar structure suitable for the vertical conduction in electronic devices. A strong (2 2 0) preferential orientation is also indicative of a low density of intra-grain defects. However, until now the electrical characterization of the films has only involved measurements of dark conductivity as a function of temperature. To ensure that the material is suitable for electronic applications, the electrical transport properties are of paramount importance.

In this work, we complement the structural characterization by using Raman spectroscopy to evaluate the crystallinity and the state of tension of the samples. In addition, we further extend the electrical characterization by performing measurements of dark conductivity and photoconductivity as function of temperature, Hall effect, ambipolar diffusion length from the steady-state photocarrier grating (SSPG) technique and the density of defects by means of modulated photoconductivity (MPC). We show that the electrical properties of our samples are comparable to or even better than those of poly-Si deposited by PECVD or HWCVD. Therefore, we suggest that these low-cost poly-Si films on glass substrates can be useful for electronic applications.

2. Experimental procedures

The CVD reactor used in this work is a batch-type, hot-wall reactor, consisting of a horizontal quartz tube located inside a tubular oven. The reaction takes place inside the quartz tube. Sheets of Schott AF37 glass, 0.3 cm thick × 0.8 cm wide × 2.5 cm long, were used as substrates. The precursor compound was $SiHCl_3$, and hydrogen was used as carrier and reaction gas. A constant flow of 38 sccm of hydrogen was made to bubble in the liquid precursor, whose temperature was kept at 0 °C. A series of runs was carried out using three substrates in each experiment. The substrates were placed one behind the other, and their location in the quartz tube (between 15 and 23 cm from the oven inlet), as well as the precursor temperature (0 °C), hydrogen flow (38 sccm) and experiment time (30 min) were kept constant for all the runs. For each run, the oven temperature was set 20 °C higher than in the previous one, starting from 760 °C and up to 880 °C, which gave rise to substrate temperatures (T_s) from 735 to 870 °C, approximately. The whole series of experiments was carried out twice in order to verify the repeatability of the results. The samples were structurally characterized by optical microscopy, SEM, AFM, reflectance spectroscopy in the UV-vis region, x-ray diffraction and Raman spectroscopy. For this last spectroscopy, we used a Witec Alpha R300 micro-Raman system operating at a wavelength of 532 nm from a solid state laser. The spot size was about 1 μm and the laser power was 0.72 mW.

Evaporated Al electrodes were deposited on top of the samples for electrical contacts, disposed in a coplanar geometry with a separation of 1 mm between them (for conductivity measurements), or at the corners of the sample in the van der Pauw configuration (for Hall effect measurements). The ohmicity of the contacts was verified. Dark conductivity and photoconductivity were measured as a function of temperature between 110 and 390 K, placing the samples inside a cryostat evacuated to a base pressure of $\sim 10^{-6}$ Torr. For the photoconductivity measurements, the sample was illuminated with a dc flux of 10^{14} cm^{-2} s^{-1} of red light (650 nm). MPC [9] was measured in the same temperature range adding a small ac flux of $\sim 3.3 \times 10^{13}$ cm^{-2} s^{-1}. At each temperature, the frequency f of the modulation was varied from 12 Hz to 40 kHz in a way such that $f_{i+1} = f_i \times 1.5$. SSPG measurements were used to evaluate the diffusion length of the minority carriers [10]. In this case, the sample was illuminated by two coherent laser beams (from a He–Ne laser) that interfere at the sample position, providing photon fluxes of 5×10^{16} and 5×10^{15} cm^{-2} s^{-1}. Finally, Hall effect measurements were performed using a magnetic field of 0.65 T. For both SSPG and Hall effect measurements, the samples were kept at room temperature.

3. Results and discussion

The basic structural characterization of the films has been presented in [7]. As a summary, we can say that the films are dense and uniform, with a good coverage and adhesion to the substrate. We obtained a deposition rate of ∼180 nm min^{-1}, a grain size of ∼0.3–0.4 μm with the columnar structure, a natural surface texture with a RMS roughness of ∼65 nm for a 3 μm thick sample, a crystalline fraction (evaluated from UV reflectance) of 70–85% and a high (2 2 0) preferential orientation (evaluated from x-ray diffraction) of ∼95 %.

3.1. Undoped samples

The structural quality of the poly-Si films can also be evaluated from Raman spectroscopy. Crystalline silicon is characterized by a sharp symmetric peak located at ∼520 cm^{-1}. A typical Raman spectrum of our films is shown in figure 1(*a*) (full line). An asymmetry in the crystalline Si peak can be noted, which can be attributed to the presence of crystallites in the nanometre range. However, the spectra do not present the broad peak at 480 cm^{-1} characteristic of amorphous silicon, and thus they can be considered truly polycrystalline.

As explained in [11], the presence of small grains (μc-Si content in the poly-Si film) gives rise to wider, less intense and red-shifted lines; the stronger the widening effect, the smaller the grains are. Consequently, this microcrystalline content contributes to the Raman spectra with a component that adds to the crystalline peak, producing the asymmetric shape. The contribution from the crystalline material can be well described by a Lorentzian function, while the contribution from the small grains is better characterized by a Gaussian function [12]. Therefore, the spectrum in figure 1 was fitted with a Lorentzian (dashed line), corresponding to the crystalline portion, and a Gaussian (dotted line) corresponding to the nanocrystalline grains. From the ratio of the areas of these two functions, we have calculated a fraction of crystalline grains, which is presented in figure 1(*b*) (right scale). As can be seen, the crystalline fraction is around 87% for the sample deposited at the lowest temperature, increases towards 93% for deposition

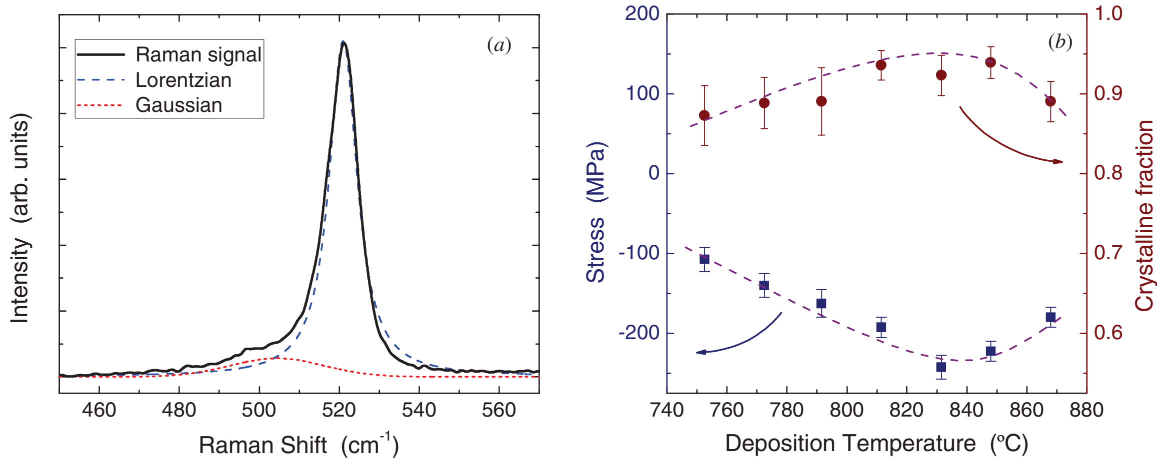

Figure 1. (*a*) Raman signal (solid line) of a typical intrinsic sample, decomposed into the contributions of the crystalline (dashed line) and nanocrystalline (dotted line) grains, and (*b*) in-plane stress, evaluated from equation (1), and crystalline fraction for the series of samples.

temperatures around 830 °C and then decreases again. This behaviour is consistent with the results obtained from UV reflectance (see figure 3 in [7]), since the crystalline fraction estimated from this method showed the same dependence on the deposition temperature.

As shown in [13, 14], Raman spectroscopy can also be used to estimate the stress present in poly-Si samples. In the case of in-plane stress, the formula is

$$\sigma\,(\mathrm{MPa}) = -250\ \Delta\omega(\mathrm{cm}^{-1}), \tag{1}$$

where $\Delta\omega = \omega_s - \omega_0$, with ω_0 being the wave number of the peak in a stress-free single crystal and ω_s being the wave number measured for the stressed sample. In this formula, a negative value corresponds to a compressive stress and a positive value to a tensile stress. In the application of this formula, care should be taken to consider other possible sources of peak shift, such as heating of the sample by the laser light or phonon confinement by small grain sizes. In the present case, the laser power was limited to avoid heating of the samples and we checked for the repeatability of the measurements. Also, the grain size of 0.3–0.4 μm implies that the peak shift due to confinement should be negligible. Figure 1(*b*) shows (left scale) the in-plane stress as a function of deposition temperature for the series of intrinsic samples. As can be seen, the compressive stress is around 100 MPa for the sample deposited at the lowest temperature, then increases up to ∼240 MPa for the sample deposited at ∼830 °C, and finally decreases again. This behaviour correlates well with the crystalline fraction, since the maximum compressive stress coincides with the maximum crystalline fraction, and also with the maximum grain size (as shown in figure 3 of [7]). Therefore, we can conclude that the nanocrystalline phase present in the samples is efficient in reducing the stress in this material.

The electrical characterization of the samples involved measurements of dark conductivity and photoconductivity as a function of temperature, modulated photoconductivity, SSPG technique, thermopower and Hall effect. For all the samples in the series, an activated behaviour of the dark conductivity has been found. Figure 2 (circles, left and bottom

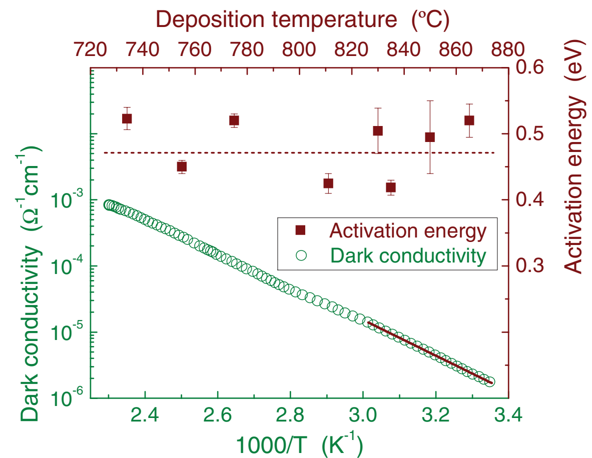

Figure 2. Dark conductivity as a function of inverse temperature for a sample deposited at $T_S \approx 830$ °C (circles, left and bottom scales), with the linear fit in the low temperature region also indicated (solid line); and activation energy as a function of deposition temperature for the series of samples (squares, top and right scales), where a fit with a constant value is also indicated (dotted line).

scales) presents an Arrhenius plot of dark conductivity as a function of inverse temperature for a sample deposited at ∼830 °C. The activation energy in this case is $E_a = 0.535$ eV and the room-temperature dark conductivity is $\sigma_{\mathrm{dk}}(25\ ^\circ\mathrm{C}) = 1.7 \times 10^{-6}\ \Omega^{-1}\ \mathrm{cm}^{-1}$. For the whole series of samples, the activation energy values are in the range of 0.42–0.54 eV, without a definite tendency as a function of deposition temperature, as can also be seen in figure 2 (squares, top and right scales). The activation energies measured for this series of samples reveal their intrinsic nature and are an indication of the absence of substantial contamination in the deposition system that we use. Thermopower measurements revealed that electrons are the majority carriers in these samples, which was further confirmed by Hall effect measurements. We obtained an electron concentration $n \cong 2 \times 10^{12}\ \mathrm{cm}^{-3}$ and a Hall mobility $\mu_H \cong 6\ \mathrm{cm}^2\ \mathrm{V}^{-1}\ \mathrm{s}^{-1}$. These values are within the range of values usually measured for high-quality

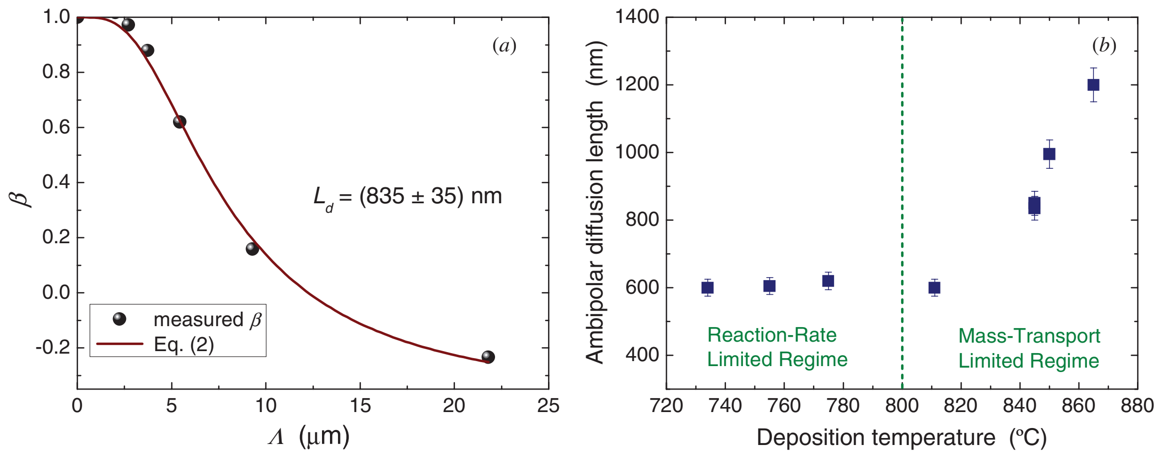

Figure 3. (*a*) SSPG measurement on a sample deposited at 835 °C (circles) and fit with equation (2) (line). (*b*) Resulting ambipolar diffusion length as a function of deposition temperature. The vertical line indicates the transition between the reaction-rate limited regime and the mass-transport limited regime.

microcrystalline silicon samples without any amorphous phase [15].

The SSPG technique has been used to measure the ambipolar diffusion length (L_d) of the samples, which is mainly determined by the minority carriers. In this technique, the ratio between the photocurrents with and without interference, β, is measured as a function of the grating period, Λ. A fit with the theoretical formula [10]

$$\beta = \frac{2\Phi}{[1 + (2\pi L_d/\Lambda)^2]^2} \tag{2}$$

allows obtaining the diffusion length. The parameter Φ takes into account the power-law dependence of the photoconductivity on the generation rate and the contrast of the grating due to experimental conditions [10]. Figure 3 presents the measurement obtained for an intrinsic sample deposited at $T_s = 845$ °C. The result is $L_d = 835$ nm, which is four to five times higher than the values usually obtained for device-quality amorphous silicon, and is also higher than the value usually quoted for device-quality microcrystalline silicon (∼500 nm) [16, 17]. Moreover, we should take into account that the measurements are performed in the coplanar configuration, and may be limited by transport through grain boundaries. An even larger diffusion length is expected along the axis of the grains. For the whole series of samples, values up to 600 nm $< L_d <$1200 nm have been obtained, as can be seen in figure 3(*b*). L_d takes a quite constant value close to 600 nm for the samples deposited in the reaction-rate-limited regime (see figure 1 of [7]), and increases with the deposition temperature for the samples deposited in the mass-transport-limited regime. An ambipolar diffusion length of 1.2 μm is a very promising value for the application of this material in electronic devices.

The density of defect states has been evaluated from MPC measurements. Figure 4 presents results of the MPC–DOS, which is given by the product Nc/μ, where N is the density of states, c is the capture coefficient of the probed states and μ is the free carrier mobility. We should recall that the DOS shape is given by the upper envelope of the MPC spectra; the deviations from this envelope coming from an influence of the

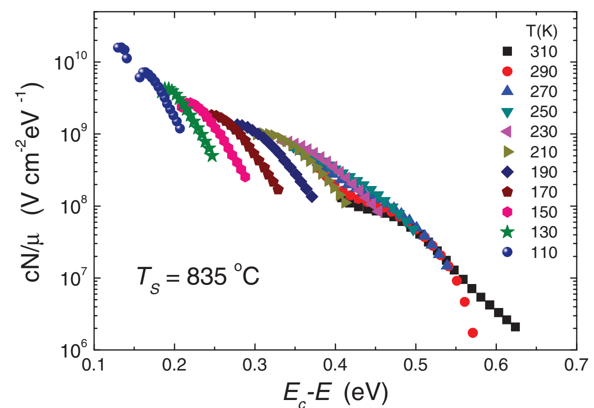

Figure 4. MPC–DOS obtained from MPC measurements performed at different temperatures indicated in the inset.

mean dc flux used to perform the experiment, as described elsewhere [18]. The MPC–DOS obtained for this sample is roughly a factor of 10 higher than what is typically obtained for hydrogenated amorphous silicon, meaning a defect density of $\sim 10^{17}$ cm^{-3} eV^{-1} in the midgap region. This is not surprising for a sample deposited at high temperature and without any defect passivation by hydrogenation.

3.2. Doped samples

In order to produce p-doped poly-Si films, we introduced in our reactor controlled amounts of BBr_3 as a boron source. The partial pressure of BBr_3 was controlled by adjusting its temperature between −35 and +30 °C, and therefore the proportion of dopant in the samples was varied. By changing the boron concentration in the samples, we obtained room-temperature dark conductivities varying between 2 × 10^{-7} Ω^{-1} cm^{-1} for the compensated samples and 15 Ω^{-1} cm^{-1} for the heavily doped samples, with activation energies between 0.61 and 0 eV, respectively. Hall effect measurements confirmed that the doped samples are p-type, with a carrier concentration that can be adjusted between

$p = 1.9 \times 10^{16}$ cm^{-3} for the lightly doped samples and $p = 3.9 \times 10^{19}$ cm^{-3} for the p^+ samples. This last value is close to those needed for the back surface field of a solar cell. On the other hand, the Hall mobilities of the p-doped samples varied between 5.6 and 14.8 cm^2 V^{-1} s^{-1}. As already mentioned, these mobilities are within the range of values usually measured for high-quality microcrystalline silicon samples without any amorphous phase [15].

In summary, a range of doping conditions—slightly n-type, compensated, slightly p-type and strongly p-type—can be obtained. The viability of doping opens the possibility of depositing thin film transistors or solar cells in a p–n or p–i–n structure.

4. Conclusions

In this work, we extended the structural and electrical characterization of thin polycrystalline silicon films deposited by thermal CVD on glass substrates. The crystalline fraction, evaluated from Raman spectroscopy, is consistent with previous results obtained from UV reflectance spectroscopy. The films exhibit compressive stress, with a dependence on deposition temperature well correlated with the crystalline fraction and the grain size. The activation energy of the dark conductivity reveals the intrinsic character of this material. The ambipolar diffusion length, evaluated from SSPG measurements, ranges between 600 and 1200 nm. This last value, which more than doubles the best results obtained for microcrystalline silicon, is an encouraging result for photovoltaic applications. The density of states in the subgap region, determined from MPC measurements, is also comparable to the values usually obtained for microcrystalline silicon.

By introducing controlled amounts of boron, we demonstrate the possibility of p-type doping. Hall effect measurements confirmed the n-type character of the undoped samples, while different degrees of p-type doping—from slightly to strongly p-type—can be achieved. The Hall mobilities range approximately between 5 and 15 cm^2 V^{-1} s^{-1}, which are typical values for microcrystalline silicon. In conclusion, our results demonstrate the feasibility of directly depositing polycrystalline silicon thin films on glass substrates by AP-CVD at intermediate temperatures for electronic or photovoltaic applications.

Acknowledgments

This work was supported by ANPCyT (Projects 22-32515 and 22-25749), CONICET (Project PIP 1464), UNL (Project CAI+D 68-349) and MINCyT—ECOS-Sud (Project A08E01).

References

[1] Suzuki T 2006 *J. Appl. Phys.* **99** 111101
[2] Beaucarne G and Slaoui A (ed) 2006 *Thin film polycrystalline silicon solar cells* in *Thin Film Solar Cells Fabrication, Characterization and Applications* ed J Poortmans and V Arkhipov chapter 3 (Chichester: Wiley)
[3] Sato K 2010 *Chem.—Asian J.* **5** 50
[4] Sato K 2009 *Nanotechnology* **20** 365207
[5] Sato K 2009 *Chem. Lett.* **38** 558
[6] Beaucarne G, Bourdais S, Slaoui A and Poortmans J 2002 *Thin Solid Films* **403–4** 229
[7] Benvenuto A G, Buitrago R H and Schmidt J A 2012 *Eur. Phys. J. Appl. Phys.* **58** 20101
[8] SCHOTT Displayglass Jena GmbH 2004 *Datasheet of glass* AF37
[9] Oheda H 1981 *J. Appl. Phys.* **52** 6693
[10] Ritter D, Weiser K and Zeldov E 1987 *J. Appl. Phys.* **62** 4563
[11] Rojas-López M, Gayou V L, Pérez-Blanco R E, Torres-Jácome A, Navarro-Contreras H and Vidal M A 2003 *Thin Solid Films* **445** 32–7
[12] Becker C, Ruske F, Sontheimer T, Gorka B, Bloeck U, Gall S and Rech B 2009 *J. Appl. Phys.* **106** 084506
[13] De Wolf I 1996 *Semicond. Sci. Technol.* **11** 139
[14] Paillard V, Puech P, Sirvin R, Hamma S and Roca i Cabarrocas P 2001 *J. Appl. Phys.* **90** 3276
[15] Schropp R E I and Zeman M 1998 *Amorphous and Microcrystalline Silicon Solar Cells: Modelling, Materials and Device Technology* (Boston, MA: Kluwer) p 54
[16] Shah A V, Meier J, Vallat-Sauvain E, Wyrsch N, Kroll U, Droz C and Graf U 2003 *Sol. Energy Mater. Sol. Cells* **78** 469
[17] Toyama T, Nishino M, Kawabe T, Sobajima Y and Okamoto H 2008 *J. Non-Cryst. Solids* **354** 2223
[18] Longeaud C and Kleider J P 1992 *Phys. Rev.* B **45** 11672